ACS OMEGA
http://pubs.acs.org/journal/acsodf
Article

Novel Sulfonanilide Inhibitors of SHIP2 Enhance Glucose Uptake into Cultured Myotubes

Mika E. A. Berg, Jette-Britt Naams,[#] Laura C. Hautala,[#] Tuomas A. Tolvanen, Jari P. Ahonen, Sanna Lehtonen, and Kristiina Wähälä*

Cite This: *ACS Omega* 2020, 5, 1430−1438
Read Online
ACCESS | Metrics & More | Article Recommendations | Supporting Information

ABSTRACT: A series of substituted sulfonanilide analogs were prepared and evaluated as novel potent inhibitors of SH2 domain-containing inositol polyphosphate 5′-phosphatase 2 (SHIP2). SHIP2 has been shown to be a new attractive target for the treatment of insulin resistance in type 2 diabetes mellitus (T2D), which can lead to life-threatening diabetic kidney disease (DKD). Amongst the synthesized compounds, the two most promising candidates, **10** and **11**, inhibited SHIP2 significantly. Additionally, these compounds induced Akt activation in a dose-dependent manner, increased the presence of glucose transporter 4 at the plasma membrane, and enhanced glucose uptake in cultured myotubes in vitro at lower concentrations than metformin, the most widely used antidiabetic drug. These results show that the novel SHIP2 inhibitors have insulin sensitizing capacity and provide prototypes for further drug development for T2D and DKD.

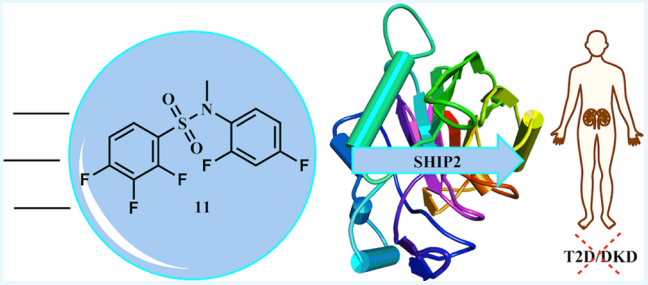

INTRODUCTION

Diabetes mellitus is one of the major health concerns in the world today. Globally, more than 425 million people were suffering from this metabolic disorder in 2017, and the predicted number of affected individuals in the future is dramatically higher, expected to reach 629 million by 2045.[1] Customarily, diabetes is divided into type 1 and type 2 diabetes mellitus (T1D and T2D) in addition to some rare forms of the disease.[2] T2D, accounting for the majority of the patients, is characterized by insulin resistance (the inability of the cells to respond to insulin) and inadequate production of insulin.[2] Severe long-term complications of T2D include cardiovascular diseases, diabetic kidney disease (DKD), diabetic retinopathy, and diabetic neuropathy.[3,4] Recently, a new classification of diabetes mellitus has been proposed, dividing the patients into five subgroups based on six clinical variables.[5] Interestingly, patients with severe insulin resistance were observed to have the highest risk of DKD, the severe and potentially life-threatening complication of diabetes.[5] This observation raises the interest to design novel insulin sensitizers that could be used to treat T2D and DKD.

At the cellular level, insulin resistance in muscle, adipose, and kidney glomerular epithelial cells may be caused by a defect in glucose uptake as a consequence of decreased activity of the phosphatidyl inositol 3 kinase (PI3K)-mediated insulin signaling pathway or impaired translocation of the insulin-responsive glucose transporter 4 (GLUT4) to the plasma membrane.[6−8] The insulin signaling cascade is activated when insulin binds to its receptor on the plasma membrane, triggering a cascade of intracellular events that result in the activation of downstream kinase Akt and glucose uptake into cells.[6] SHIP2, SH2 domain-containing inositol polyphosphate 5′-phosphatase 2, has been identified as a 5′-lipid phosphatase that suppresses insulin signaling by hydrolyzing the PI3K product PtdIns(3,4,5)P_3 (PIP_3) to PtdIns(3,4)P_2 (PIP_2), resulting in a reduced activation of Akt and diminished glucose uptake.[9,10] Both genetic and experimental studies link SHIP2 to metabolic disorders. Polymorphisms in *INPPL1*, the gene encoding SHIP2, are associated with hypertension, the metabolic syndrome, and T2D.[11−15] In rodent models of insulin resistance and T2D, SHIP2 has been shown to be upregulated in insulin responsive tissues, including the skeletal muscle, adipose tissue, and kidney glomeruli,[16,17] apparently contributing to insulin resistance. In addition, a transgenic mouse model overexpressing SHIP2 under a modified β-actin promoter impairs glucose tolerance and insulin sensitivity.[13] These data indicate that SHIP2 is an excellent drug target to ameliorate insulin resistance and treat T2D and DKD.

Only a few compounds that inhibit SHIP2 have been described. The known inhibitors belong to the thienylamide-based,[18,19] pyridinylamide-based,[20] or (benzenesulfonylamino)benzamide-based[21] compound classes.

Received: September 10, 2019
Accepted: December 30, 2019
Published: January 14, 2020

https://dx.doi.org/10.1021/acsomega.9b02944
ACS Omega 2020, 5, 1430−1438

Scheme 1. Synthesis of SHIP2 Sulfonanilide Inhibitors[a]

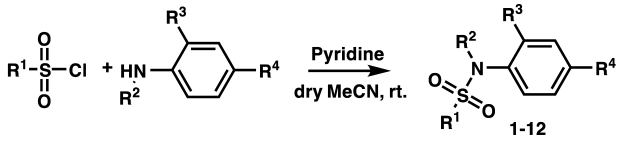

Entry	R^1	R^2	R^3	R^4	Time (min.)	Yield* (%)	Purity** (%)
1	Phenyl	Me	H	H	45	68	100
2	4-Tolyl	Me	H	H	40	67	100
3	2-Naphthyl	Me	H	H	35	55	99.9
4	2,3,4-Trifluorophenyl	Me	H	H	150	57	100
5	3-Furyl	Me	H	H	90	53	98.2
6	2-Thienyl	Me	H	H	60	64	99.5
7	4-Tolyl	H	Br	F	150	56	100
8	2,3,4-Trifluorophenyl	H	Br	F	150	50	100
9	3-Furyl	H	Br	F	210	49	100
10	2-Thienyl	H	Br	F	120	51	99.6
11	2,3,4-Trifluorophenyl	Me	F	F	120	58	99.7
12	2-Thienyl	Me	F	F	270	64	99.3

[a]Reagents and conditions: sulfonyl chloride (1 equiv), aniline or *N*-methylaniline derivative (1 equiv), pyridine (~6 equiv), dry MeCN (5 mL), room temperature, 35−210 min. *Yield is calculated after recrystallization from MeOH or EtOH. **Purity is determined using HPLC by careful integration of the peak areas.

Furthermore, only a few studies describe the effects of these inhibitors in animal models or cultured cells.[19−21] We recently observed that metformin, a biguanide, binds to SHIP2 directly and inhibits its catalytic activity,[22] thus supporting SHIP2 as a target to treat T2D. Apart from metformin, none of the other thus far described SHIP2 inhibitors are in clinical use. We have now designed a sulfonanilide-based compound library of new SHIP2 inhibitors and tested their potency to inhibit SHIP2 in vitro. In addition, using cultured myotubes, we tested whether the two most potent inhibitors enhance the activation of the insulin signaling pathway and increase glucose uptake.

RESULTS

Chemistry. Various novel sulfonanilide SHIP2 inhibitor candidates (**1**−**12**) were synthesized by stirring together different sulfonyl chlorides with various anilines or *N*-methylanilines under basic conditions in acetonitrile at room temperature. The solid sulfonanilide products were obtained in good yields (49−68%) and high purity (>98%) after recrystallization (Scheme 1).

Inhibition of SHIP2 Activity by Sulfonanilides. To investigate the ability of the sulfonanilides to inhibit the activity of SHIP2, we divided them to three groups based on three different anilines: *N*-methylaniline, 2-bromo-4-fluoroaniline, and 2,4-difluoro-*N*-methylaniline. The *N*-methylaniline-based sulfonanilides **1**−**6** inhibited SHIP2 activity by only 3−15% (Table 1). Replacing *N*-methylaniline with 2-bromo-4-fluoroaniline resulted in the *p*-tolyl compound **7**, which inhibited SHIP2 activity by 17%. On the other hand, a slight decrease in the inhibition was seen for the trifluorophenyl compound **8** and furyl compound **9**, which inhibited SHIP2 activity by 10 and 9%, respectively. In contrast, the 2-thienyl-substituted analog **10** showed an increase in the SHIP2 inhibition, with a very promising inhibition efficiency of 45%. Alternatively, modifying the aniline in compound **8** to 2,4-difluoro-*N*-methylaniline gave an increase in the inhibition for the pentafluorinated compound **11**, which similarly inhibited SHIP2 activity by 45%. The 2-thienyl compound **12** with 2,4-difluoro-*N*-methylaniline was almost inactive. The IC_{50} values for the best two SHIP2-inhibiting sulfonanilides, **10** and **11**, were 41.2and 7.07 μM, respectively (Table 1).

Table 1. IC_{50} Values and Maximal Inhibition of Sulfonanilide Analogs 1−12

entry	IC_{50} (μM)	max. inhibition (%)
1	NA[a]	6 ± 2.8
2	NA[a]	10 ± 7.2
3	>50	15 ± 1.6
4	>50	12 ± 4.0
5	NA[a]	3 ± 1.5
6	>50	11 ± 2.2
7	>50	17 ± 2.1
8	NA[a]	10 ± 5.1
9	NA[a]	9 ± 3.0
10	41.2	45 ± 17
11	7.07	45 ± 0.7
12	NA[a]	5 ± 1.7

[a]IC_{50} values not assigned (NA) for compounds with inhibition equal or lower than 10%.

Cytotoxicity of Sulfonanilides 10 and 11. To further evaluate the properties of the sulfonanilides **10** and **11**, we measured whether they affect the viability of L6 myotubes using the alamarBlue cell viability assay. Sulfonanilides **10** and **11** showed no or very little effect on cell viability up to 200 μM concentration (Figure 1). When the concentration was increased to 300 μM, sulfonanilide **10** decreased the viability of myotubes by only 7% whereas sulfonanilide **11** reduced cell

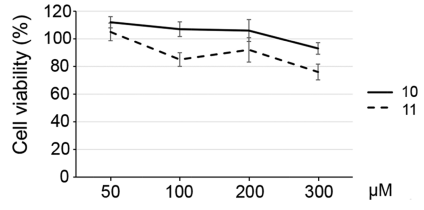

Figure 1. Cytotoxicity of sulfonanilides **10** and **11**. Sulfonanilide **10** was not cytotoxic up to 200 μM concentration. Both sulfonanilides **11** and **10** affected very little the cytotoxicity at high concentrations (tested up to 300 μM).

https://dx.doi.org/10.1021/acsomega.9b02944
ACS Omega 2020, 5, 1430−1438

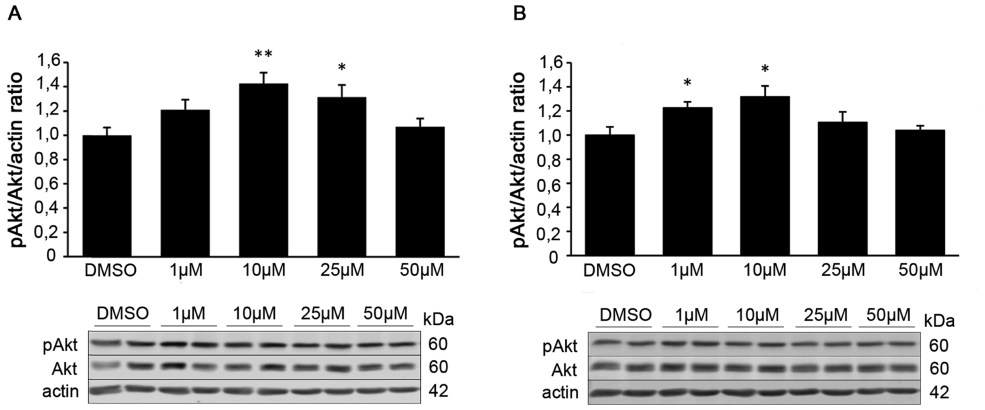

Figure 2. Sulfonanilides **10** and **11** activate Akt in L6 myotubes. L6 myotubes serum starved for 20 h were treated with sulfonanilide **10** or **11** (1−50 μM) or vehicle (DMSO) for 15 min after which insulin (10 nM) was added for an additional 15 min. Activation of the insulin signaling pathway was determined by analyzing the phosphorylation of Akt at Ser473 by quantitative Western blotting. (A, B) Quantification of protein levels of three replicate Western blots of L6 myotubes treated with (A) **10** or (B) **11** and representative blots. Data are expressed as fold-change relative to the vehicle, and values are mean ± SEM. Three experiments in which $n = 3$ for each condition. *$p < 0.05$, **$p < 0.01$.

viability by 24% at this concentration (Figure 1). This indicates that sulfonanilides **10** and **11** are not toxic to myotubes.

Sulfonanilides 10 and 11 Activate the Insulin Signaling Pathway. As the phosphorylation of Akt indicates the activation of the insulin signaling pathway, we next determined the effect of sulfonanilides **10** and **11** on insulin-induced Akt phosphorylation in L6 myotubes. For this, myotubes were pretreated for 15 min with 1, 10, 25, or 50 μM sulfonanilide **10** or **11** followed by stimulation with 10 nM insulin for an additional 15 min. Akt was activated with 10 and 25 μM sulfonanilide **10** and 1 and 10 μM sulfonanilide **11** (Figure 2). Neither sulfonanilide **10** nor **11** activated Akt at 50 μM concentration in this short-term treatment. The level of total Akt did not change under any of the conditions (Figure 2). These data indicate that sulfonanilides **10** and **11** increase insulin-induced phosphorylation of Akt in a dose-dependent manner in a short-term treatment.

Sulfonanilides 10 and 11 Enhance Glucose Uptake. To determine the functional effects of sulfonanilides **10** and **11**, we evaluated their ability to enhance glucose uptake into L6 myotubes stably overexpressing HA-tagged GLUT4 glucose transporter (referred to as L6-GLUT4 myotubes).[18] For this, L6-GLUT4 myotubes were treated with 50 μM sulfonanilide **10** or **11** for 20 h, whereafter the cells were treated or not with 100 nM insulin, followed by measuring the cellular uptake of radioactively labeled 2-deoxyglucose. For comparison, we carried out glucose uptake assays with metformin, the previously characterized SHIP2 inhibitor,[22] using the same 50 μM concentration of metformin. Under serum starvation, both **10** and **11** alone increased glucose uptake by 18−19%. With insulin stimulation, **10** and **11** increased glucose uptake by 30 and 23%, respectively, compared to control cells stimulated with insulin (Figure 3). Metformin, on the other hand, did not enhance glucose uptake at this concentration with or without insulin stimulation (Figure 3). These data indicate that sulfonanilides **10** and **11** enhance insulin-induced glucose uptake into L6-GLUT4 myotubes at 50 μM concentration whereas metformin does not.

Sulfonanilides 10 and 11 Increase the Presence of GLUT4 at the Plasma Membrane. To further confirm that sulfonanilides **10** and **11** affect the insulin signaling pathway, we investigated their effect on GLUT4 translocation, using L6-GLUT4 myotubes. The HA-tag is located in the extracellular

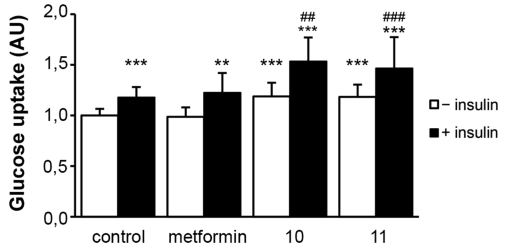

Figure 3. Sulfonanilides **10** and **11** enhance glucose uptake in L6 myotubes. Glucose uptake in L6 myotubes overexpressing GLUT4 transporter was measured by a radioactive 2-deoxyglucose assay after 20 h serum starvation and inhibitor treatment (sulfonanilides **10** or **11**, or metformin) and either with or without 15 min insulin stimulation. Four experiments in which $n = 4$ for each condition. Data are expressed as fold-change relative to the control (no inhibitor treatment, no insulin), and values are mean ± STD. Statistical significance denoted as: * = compared to control without insulin; # = compared to control with insulin; **/## $p \leq 0.01$, ***/### $p \leq 0.001$ (unpaired Student's t-test).

domain of GLUT4, which allows quantifying the presence of GLUT4 on the plasma membrane by surface labeling with an antibody against the HA-tag. In control myotubes without sulfonanilide treatment, insulin stimulation increased the relative amount of GLUT4 on the plasma membrane by 16% compared to myotubes without insulin treatment (Figure 4). Treatment of myotubes with sulfonanilide **10** led to a 4% increase in the amount of GLUT4 on the plasma membrane without insulin stimulation (Figure 4). The increase with insulin stimulation was 26% compared to control cells without insulin stimulation and 10% compared to control cells treated with insulin. Sulfonanilide **11** increased the presence of GLUT4 on the plasma membrane by 8% without insulin stimulation. The increase with insulin stimulation was 15% compared to control cells without insulin stimulation, but when compared to control cells with insulin stimulation, there was no increase (Figure 4).

Docking Studies of Sulfonanilide 11. To investigate the binding mode of our most potent inhibitor, sulfonanilide **11**, we docked **11** onto the phosphatase domain of SHIP2 (PDB ID: 4A9C; crystal structure described by Mills et al.[23]) (Figure 5). In our simulations, the sulfonyl group binds tightly between the four amino acid units Arg 611, Tyr 661, Arg 682, and Asn

https://dx.doi.org/10.1021/acsomega.9b02944
ACS Omega 2020, 5, 1430−1438

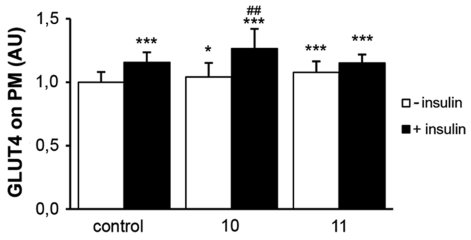

Figure 4. Sulfonanilides **10** and **11** increase the presence of GLUT4 on the plasma membrane. HA-GLUT4 on the plasma membrane (PM) was measured by On-Cell Western assay after 20 h treatment with sulfonanilide **10** or **11** and either with or without 15 min insulin stimulation. Four experiments in which $n = 6-10$ for each condition. Data are expressed as fold-change relative to the control (no sulfonanilide treatment, no insulin), and values are mean ± STD. Statistical significance denoted as: * = compared to control without insulin; # = compared to control with insulin; */# $p \leq 0.05$, **/## $p \leq 0.01$, ***/### $p \leq 0.001$ (unpaired Student's t-test).

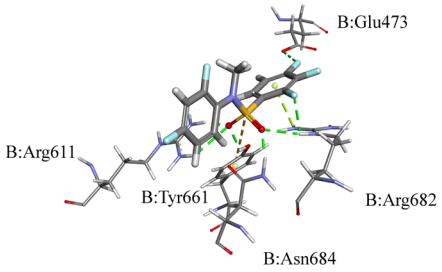

Figure 5. Molecular docking analysis of sulfonanilide **11** onto the binding pocket of the SHIP2 phosphatase domain (PDB ID: 4A9C).

684 in SHIP2. The fluoride substituents are hydrogen bonded to Arg 682 and Glu 473. Additionally, π-stacking is observed from the phenyl ring to the Arg 682 unit.

DISCUSSION

We have designed and synthesized a series of sulfonanilide derivatives that we analyzed for their potency to act as novel SHIP2 inhibitors. Based on our in vitro analyses, we have created two new nontoxic SHIP2 inhibitors that enhance glucose uptake into cultured myotubes more potently than metformin.

In our molecular library of 12 sulfonanilide derivatives, based on three different anilines, we observed that combining a highly fluorinated benzenesulfonyl chloride with 2,4-difluoro-*N*-methylaniline as in **11** increases the ability of the sulfonanilide to inhibit the activity of SHIP2 as measured by using the purified SHIP2 phosphatase domain and malachite green phosphate assay. Additionally, the 2-thienyl compound **12** with 2,4-difluoro-*N*-methylaniline was almost inactive possibly due to blocking of the hydrogen bonding to the free N−H group, therefore having a negative effect on the binding mode. This result indicates that 2-bromo-4-fluoroaniline should be preferably combined with a heteroarenesulfonyl chloride as seen in **10**, which increases the ability of the compound to inhibit SHIP2. Consequently, sulfonanilides **10** and **11** were identified as the most potent SHIP2 inhibitors.

As SHIP2 hydrolyzes PIP_3 to PIP_2 and thereby reduces the activation of Akt,[9,10] SHIP2 inhibition is expected to lead to the activation of Akt. In line with this, we observed that sulfonanilides **10** and **11** increase the insulin-induced phosphorylation of Akt, indicative of its activation, in a similar manner as the previously characterized SHIP2 inhibitors AS1949490, AS1938909, and *N*-[4-(4-chlorobenzyloxy)-pyridine-2-yl]-2-(2,6-difluorophenyl)-acetamide (CPDA).[18−20] Sulfonanilides **10** and **11** activated Akt in a dose-dependent manner, with the lowest concentrations (10 and 25 μM for **10** and 1 and 10 μM for **11**) enhancing Akt phosphorylation in a short-term (30 min) treatment. The highest concentration tested (50 μM) did not enhance Akt activation in this short-term treatment, apparently indicative of activation of a negative feedback loop abolishing Akt activation. In the cell viability measurements using alamarBlue, which measures cellular metabolism and cell viability,[24,25] both **10** and **11** appeared to slightly enhance the metabolic activity of the cells at 50 μM concentration. The highest concentration of sulfonanilide **11** (300 μM) lowered cell viability by 24% while **10** had only a minor effect on viability at this concentration. This indicates that both **10** and **11** are well tolerated by myotubes at their effective concentrations.

SHIP2 inhibition is expected to enhance the insulin-induced increase in glucose uptake, and as expected, sulfonanilides **10** and **11** increased glucose uptake into myotubes after 20 h treatment at 50 μM concentration. Metformin, the most widely used antidiabetic drug, did not increase glucose uptake at this concentration. We and others have previously shown that 2 mM metformin is necessary to increase glucose uptake into myotubes.[22,26] It may be that sulfonanilides **10** and **11** are more potent than metformin in increasing glucose uptake, or alternatively, **10** and **11** may be transported more efficiently into cells than metformin. Metformin is internalized by organic cation transporters (OCTs), the expression of which is lowered in cultured cells in vitro compared to tissues in vivo, thus leading to a low uptake of metformin in vitro.[27] Previous studies have shown that sulfonylureas bind to the sulfonylurea receptor (SUR) subunit of the ATP-sensitive potassium channel, also present in muscle cells.[28] Apparently, sulfonanilides **10** and **11** are internalized in a similar manner by SUR, but this requires further studies. Nevertheless, sulfonanilides **10** and **11** enhanced insulin-stimulated glucose uptake into myotubes at a concentration ineffective for metformin.

An earlier study revealed that the sulfonylureas gliclazide and glyburide increased glucose uptake independently of insulin by increasing the content of glucose transporter 1 (GLUT1) at the plasma membrane in L6 myotubes, with no effect on GLUT4.[29] Sulfonanilides **10** and **11** slightly increased the presence of GLUT4 on the plasma membrane with or without insulin stimulation, which may be due to increased exocytosis or slower endocytosis of GLUT4 as a result of the treatment with the sulfonanilides. This may explain at least partially the increased glucose uptake seen with sulfonanilides **10** and **11**. On the other hand, the sulfonylureas glimepiride, gliquidone, and glipizide have been shown to enhance insulin sensitivity of 3T3-L1 adipocytes by increasing the transcriptional activity of the peroxisome proliferator-activated receptor γ (PPARγ),[30] a transcription factor that regulates lipid and glucose metabolism.[31] It thus appears that different sulfonylureas affect glucose metabolism via different mechanisms, in addition to their major function as enhancers of insulin secretion from pancreatic β-cells.[27]

The new suggested classification of diabetes into different subgroups based on specific clinical characteristics opens an important avenue for developing new and more effective individualized treatments as patients in different subgroups have a differing risk of diabetic complications.[5] Of special

https://dx.doi.org/10.1021/acsomega.9b02944
ACS Omega 2020, 5, 1430−1438

interest in terms of DKD is the subgroup of severely insulin resistant patients.[5] In our previous study, we found that SHIP2 activity is elevated in the kidney in patients with T2D receiving other medication than metformin compared to people without diabetes.[22] We further found that metformin increases the insulin sensitivity of peripheral tissues and protects from a kidney injury by inhibiting the catalytic activity of SHIP2.[22] Thus, new SHIP2 inhibitors that are more potent than metformin in their insulin sensitizing capacity could provide more effective treatment options for T2D and DKD and serve as an alternative to metformin when its use is contraindicated.

In conclusion, our results show the potential of targeting SHIP2 to develop new treatments for T2D. Here, we have synthesized a molecular library of sulfonanilide derivatives and established their capacity to act as novel SHIP2 inhibitors. Among the compounds synthesized, 2′-bromo-4′-fluoro-2-thiophenesulfonanilide (**10**) and 2′,4′-difluoro-*N*-methyl-2,3,4-trifluorobenzenesulfonanilide (**11**) were identified as the most potent SHIP2 inhibitors having insulin sensitizing capacities. Therefore, these compounds serve as important prototypes for the further development of new treatments for T2D and DKD.

EXPERIMENTAL SECTION

Materials and Methods. Commercially purchased reagents and solvents were used without further purification if not otherwise stated. *N*-Methylaniline and 2-bromo-4-fluoroaniline were distilled prior to use. The solvents were dried in a VAC Vacuum Atmospheres Co. solvent purifier system. The reactions were followed using Sigma-Aldrich Supelco silica gel on TLC Al foils with fluorescent indicator 254 nm and using the Plate Express Advion MS (TLC-CMS) instrument with APCI±-ionization. Column chromatography was performed using VWR Chemicals silica gel 40−60 μm with the eluent systems specified in the experiments. Melting points were measured in one end open capillaries with a digital melting point apparatus, Büchi B-545. ^{1}H and ^{13}C-NMR spectra were recorded on a Varian UNITY INOVA 500 spectrometer (500 MHz ^{1}H-frequency and 125 MHz ^{13}C-frequency) in $CDCl_3$ (containing 0.03% tetramethylsilane, TMS, as reference) or DMSO-d_6 as a solvent at 27 °C. All the chemical shifts are given in parts per million (ppm). IR spectra were recorded using a Bruker ALPHA FT-IR spectrometer with a platinum-ATR disc (Bruker Optics). High-resolution mass spectrometry, HRMS, analyses were made using a Bruker Micro-TOF time-of-flight mass spectrometer (Bruker Daltonics) with positive electrospray ionization (ESI+). The protonated molecular ion, $[M + H^+]$, or the corresponding sodium salt, $[M + Na + H^+]$, was identified. All the measured HRMS *m*/*z*-values were within a 5 ppm error margin.

The purity of the final products was determined using reversed-phase high-performance liquid chromatography, RP-HPLC. The purity of all compounds was above 98%, determined by integration of the peak areas using an Agilent 1200 series LC-unit. The column used was a Waters Symmetry RP-C_{18}, 5 microns particle size, 4.6 mm × 250 mm. The products were eluted with the MeCN/0.1% formic acid in milli-Q water eluent mixture using a gradient method (55:45 0−4 min, 55:45 to 90:10 4−14 min, 90:10 to 55:45 14−19 min, 55:45 19−25 min). The flow rate was 1 mL min^{-1} (pressure ∼110 bar), and UV-wavelengths used were 254, 280, and 265 nm. The column temperature was 40 °C, and the injection volume was 10 μL. Elemental analyses were performed on a vario MICRO cube elemental analyzer (Elementar Analysensysteme GmbH, Hanau, Germany).

General Procedure for the Synthesis of Compounds 1−12. In our protocol for preparing the sulfonanilides, the sulfonyl chloride (1 equiv) was dissolved in dry acetonitrile (5 mL) under argon atmosphere at room temperature. The aniline or *N*-methylaniline (1 equiv) in pyridine (∼6 equiv) was added to the sulfonyl chloride solution. The reaction was stirred at room temperature under argon and monitored by TLC and TLC-CMS until completion (35−270 min). The reaction mixture was acidified with aq 2 M HCl solution and extracted with ethyl acetate (6 × 5 mL). The organic layer was separated, washed with 30 mL of water and 30 mL of aq sat NaCl solution, dried over $MgSO_4$, filtered, and evaporated. The crude solid product was purified by recrystallization from either methanol or ethanol (abs). The pure solid product was filtered, dried, and characterized by spectroscopic methods.

N-Methylbenzenesulfonanilide (**1**). For full structural characterization and chemical properties, see the Supporting Information.

N-Methyl-*p*-toluenesulfonanilide (**2**). For full structural characterization and chemical properties, the see Supporting Information.

N-Methyl-2-naphthalenesulfonanilide (**3**). For full structural characterization and chemical properties, see the Supporting Information.

N-Methyl-2,3,4-trifluorobenzenesulfonanilide (**4**). White needles; yield 57%; mp 104 °C (EtOH). ^{1}H NMR (500 MHz, $CDCl_3$): δ_H 7.43−7.38 (m, 1H), 7.34−7.26 (m, 3H), 7.19−7.16 (m, 2H), 7.01 (tdd, *J* = 9.01 Hz, 6.57 Hz, 2.10 Hz, 1H), 3.37 ppm (d, *J* = 1.96 Hz, 3H). ^{13}C NMR (125 MHz, $CDCl_3$): δ_C 154.32 (ddd, 258.90 Hz, 9.80 Hz, 3.08 Hz, C−F), 148.98 (ddd, 260.00 Hz, 11.64 Hz, 4.08 Hz, C−F), 140.61 (dt, 256.68 Hz, 15.57 Hz, C−F), 140.58 (C_{quat}), 129.51, 128.13, 126.88, 125.73 (dd, 8.51 Hz, 4.40 Hz, C−H_{arom}), 124.06 (ddd, 12.06 Hz, 4.06 Hz, 2.12 Hz, C_{quat}), 112.45 (dd, 17.94 Hz, 3.89 Hz, C−H_{arom}), 38.84 ppm (d, *J* = 3.48 Hz, CH_3). IR (cm^{-1}): $\tilde{\nu}$ = 3064 (s; ν(C−H_{arom})), 2987 (s; ν(C−H_{aliph})), 2943 (s; ν(C−H_{aliph})), 1603 (m), 1503 (m), 1455 (m), 1354 (s; ν(SO_2−N)), 1154 (s; ν(SO_2−N)), 1123 (s; ν(C−F)), 1034 (s), 701 (s). HRMS (ESI): *m*/*z* calcd for $C_{13}H_{10}F_3NO_2S + H^+$ $[M + H^+]$: 302.0457. Found: 302.0442. HPLC analysis: retention time = 10.908 min, peak area, 100%. Elemental analysis calcd (%) for $C_{13}H_{10}F_3NO_2S$: C 51.83, H 3.35, N 4.65, S 10.64. Found: C 51.76, H 3.37, N 4.69, S 10.63.

N-Methyl-3-furansulfonanilide (**5**). White needles; yield 53%; mp 100 °C (MeOH). ^{1}H NMR (500 MHz, $CDCl_3$): δ_H 7.73 (s, 1H), 7.45 (t, *J* = 1.54 Hz, 1H), 7.35−7.26 (m, 3H), 7.21−7.19 (m, 2H), 6.34 (d, *J* = 1.54 Hz, 1H) 3.22 ppm (s, 3H). ^{13}C NMR (125 MHz, $CDCl_3$): δ_C 146.15 (CH−O), 144.52 (CH−O), 141.47 (C_{quat}), 129.21, 127.80, 126.82, 123.91 (C_{quat}), 109.24, 38.28 ppm (CH_3). IR (cm^{-1}): $\tilde{\nu}$ = 3156 (s; ν(furan)), 3135 (s; ν(furan)), 3009 (s; ν(C−H_{arom})), 2980 (s; ν(C−H_{aliph})), 1595 (m), 1492 (s), 1369 (s; ν(SO_2−N)), 1157 (s; ν(SO_2−N)), 1130 (s), 1009 (s; ν(furan)), 870 (s, ν(furan)), 816 (s). HRMS (ESI): *m*/*z* calcd for $C_{11}H_{11}NO_3S + H^+$ $[M + H^+]$: 238.0532. Found: 238.0522. HPLC analysis: retention time = 6.795 min, peak area, 98.2%. Elemental analysis calcd (%) for $C_{11}H_{11}NO_3S$: C 55.68, H 4.67, N 5.90, S 13.51. Found: C 55.42, H 4.68, N 5.92, S 13.50.

N-Methyl-2-thiophenesulfonanilide (**6**). For full structural characterization and chemical properties, see the Supporting Information.

https://dx.doi.org/10.1021/acsomega.9b02944
ACS Omega 2020, 5, 1430−1438

2′-Bromo-4′-fluoro-*p*-toluenesulfonanilide (**7**). For full structural characterization and chemical properties, see the Supporting Information.

2′-Bromo-4′-fluoro-2,3,4-trifluorobenzenesulfonanilide (**8**). After work-up, the crude product was purified by column chromatography on silica gel using *n*-hexane/dichloromethane (1:1) followed by recrystallization. White solid; yield 50%; mp 83 °C (EtOH). ^{1}H NMR (500 MHz, $CDCl_3$): δ_H 7.62 (dd, J = 9.15 Hz, 5.24 Hz, 1H), 7.55 (tdt, J = 6.92 Hz, 3.20 Hz, 2.42 Hz, 1H), 7.23 (dd, J = 7.64 Hz, 2.81 Hz, 1H), 7.10 (bs, 1H, N−H), 7.07−7.01 ppm (m, 2H). ^{13}C NMR (125 MHz, $CDCl_3$): δ_C 160.28 (d, J = 251.44 Hz, C−F), 154.97 (ddd, J = 259.72 Hz, 10.11 Hz, 3.27 Hz, C−F), 149.11 (ddd, J = 260.99 Hz, 11.79 Hz, 4.05 Hz, C−F), 140.66 (dt, J = 257.88 Hz, 15.47 Hz, C−F), 130.19 (d, J = 3.70 Hz, C_{quat}), 125.53 (d, J = 8.66 Hz, C−H), 125.10 (dd, J = 8.80 Hz, 4.47 Hz, $C-H_{arom}$), 124.90 (ddd, J = 11.13 Hz, 3.81 Hz, 1.66 Hz, C_{quat}), 120.26 (d, J = 25.78 Hz, $C-H_{arom}$), 117.09 (d, J = 9.80 Hz, C_{quat}), 116.06 (d, J = 22.28 Hz, $C-H_{arom}$), 112.69 ppm (dd, J = 18.23 Hz, 3.84 Hz, $C-H_{arom}$). IR (cm^{-1}): $\tilde{\nu}$ = 3259 (s; ν(N−H)), 3088 (s; $\nu(C-H_{arom})$), 1596 (m), 1487 (m), 1347 (s; $\nu(SO_2-N)$), 1168 (s; $\nu(SO_2-N)$), 1038 (s; ν(C−F)), 819 (s), 598 (s; ν(C−Br)). HRMS (ESI): m/z calcd for $C_{12}H_5BrF_4NO_2S$ + Na + H^+ [M + Na + H^+]: 405.9131. Found: 405.9119. HPLC analysis: retention time = 10.377 min, peak area, 100%. Elemental analysis calculated (%) for $C_{12}H_5BrF_4NO_2S$: C 37.52, H 1.57, N 3.65, S 8.35. Found: C 37.31, H 1.71, N 3.66, S 8.38.

2′-Bromo-4′-fluoro-3-furansulfonanilide (**9**). White solid; yield 49%; mp 126 °C (EtOH). ^{1}H NMR (500 MHz, $CDCl_3$): δ_H 7.79 (dd, J = 1.73 Hz, 0.75 Hz, 1H), 7.67 (dd, J = 8.93 Hz, 5.33 Hz, 1H), 7.41 (t, J = 1.73 Hz, 1H), 7.24 (dd, J = 7.70 Hz, 2.88 Hz, 1H), 7.06 (ddd, J = 8.93 Hz, 7.84 Hz, 2.88 Hz, 1H), 6.88 (bs, 1H, N−H), 6.50 ppm (dd, J = 1.73 Hz, 0.75 Hz, 1H). ^{13}C NMR (125 MHz, $CDCl_3$): δ_C 160.12 (d, J = 251.01 Hz, C−F), 146.42 (CH−O), 144.94 (CH−O), 130.97 (d, J = 3.52 Hz, C_{quat}), 126.20 (C_{quat}), 125.33 (d, J = 8.87 Hz, $C-H_{arom}$), 120.08 (d, J = 25.88 Hz, $C-H_{arom}$), 117.22 (d, J = 10.13 Hz, C_{quat}), 116.00 (d, J = 22.48 Hz, $C-H_{arom}$), 108.55 ppm. IR (cm^{-1}): $\tilde{\nu}$ = 3258 (s; ν(N−H)), 3147 (s; ν(furan)), 3129 (s; ν(furan)), 3092 (s; $\nu(C-H_{arom})$), 1599 (m), 1485 (s), 1330 (s; $\nu(SO_2-N)$), 1194 (s; $\nu(SO_2-N)$), 1151 (s; ν(C−F)), 1005 (s; ν(furan)), 872 (s, ν(furan)), 821 (s), 601 (s; ν(C−Br)). HRMS (ESI): m/z calcd for $C_{10}H_6BrFNO_3S$ + Na + H^+ [M + Na + H^+]: 341.9206. Found: 341.9197. HPLC analysis: retention time = 6.707 min, peak area, 100%. Elemental analysis calcd (%) for $C_{10}H_6BrFNO_3S$: C 37.52, H 2.20, N 4.38, S 10.01. Found: C 37.46, H 2.17, N 4.48, S 10.17.

2′-Bromo-4′-fluoro-2-thiophenesulfonanilide (**10**). Off-white solid; yield 51%; mp 109 °C (EtOH). ^{1}H NMR (500 MHz, $CDCl_3$): δ_H 7.70 (dd, J = 9.03 Hz, 5.37 Hz, 1H), 7.58 (dd, J = 4.99 Hz, 1.31 Hz, 1H), 7.45 (dd, J = 3.82 Hz, 1.31 Hz, 1H), 7.21 (dd, J = 7.70 Hz, 2.87 Hz, 1H), 7.07 (ddd, J = 9.03 Hz, 7.71 Hz, 2.87 Hz, 1H), 7.02 (dd, J = 4.99 Hz, 3.82 Hz, 1H) 6.88 ppm (bs, 1H, N−H). ^{13}C NMR (125 MHz, $CDCl_3$): δ_C 160.23 (d, J = 251.00 Hz, C−F), 139.05 (C_{quat}), 133.34 (CH−S), 133.29, 130.98 (d, J = 3.27 Hz, C_{quat}), 127.74, 126.04 (d, J = 8.68 Hz, $C-H_{arom}$), 119.97 (d, J = 26.14 Hz, $C-H_{arom}$), 117.81 (d, J = 9.93 Hz, C_{quat}), 115.99 ppm (d, J = 21.92 Hz, $C-H_{arom}$). IR (cm^{-1}): $\tilde{\nu}$ = 3257 (s; ν(N−H)), 3089 (s; ν(thiophene)), 1596 (m), 1483 (m), 1335 (s; $\nu(SO_2-N)$), 1156 (s; $\nu(SO_2-N)$), 1037 (s; ν(C−F)), 873 (s), 731 (s; ν(thiophene)), 567 (s; ν(C−Br)). HRMS (ESI): m/z calcd for $C_{10}H_6BrFNO_2S_2$ + Na + H^+ [M + Na + H^+]: 357.8978. Found: 357.8973. HPLC analysis: retention time = 8.024 min, peak area, 99.6%. Elemental analysis calcd (%) for $C_{10}H_6BrFNO_2S_2$: C 35.73, H 2.10, N 4.17, S 19.07. Found: C 35.65, H 2.09, N 4.32, S 19.11.

2′,4′-Difluoro-*N*-methyl-2,3,4-trifluorobenzenesulfonanilide (**11**). White solid; yield 58%; mp 106 °C (EtOH). ^{1}H NMR (500 MHz, $CDCl_3$): δ_H 7.50−7.45 (m, 1H), 7.38 (td, J = 8.78 Hz, 5.87 Hz, 1H), 7.03 (tdd, J = 9.94 Hz, 4.66 Hz, 2.10 Hz, 1H), 6.89 (dddd, J = 8.78 Hz, 7.38 Hz, 2.80 Hz, 1.43 Hz, 1H), 6.80 (ddd, J = 10.61 Hz, 8.32 Hz, 2.80 Hz, 1H), 3.35 ppm (q, J = 0.96 Hz, 3H). ^{13}C NMR (125 MHz, $CDCl_3$): δ_C 162.79 (dd, J = 252.30 Hz, 11.78 Hz, C−F), 159.81 (dd, J = 254.44 Hz, 12.80 Hz, C−F), 154.53 (ddd, J = 259.26 Hz, 19.88 Hz, 2.82 Hz, C−F), 149.19 (ddd, J = 260.97 Hz, 11.52 Hz, 3.81 Hz, C−F) 140.70 (dt, J = 241.16 Hz, 15.62 Hz, C−F), 133.23 (dd, J = 10.22 Hz, 2.51 Hz, $C-H_{arom}$), 125.31 (dd, J = 8.67 Hz, 4.45 Hz, $C-H_{arom}$), 124.94 (m, C_{quat}), 123.79 (dd, J = 12.21 Hz, 4.24 Hz, C_{quat}), 112.42 (d, J = 3.76 Hz, $C-H_{arom}$), 112.26 (t, J = 3.88 Hz, $C-H_{arom}$), 105.25 (dd, J = 26.43 Hz, 23.67 Hz, $C-H_{arom}$), 38.75 ppm (t, J = 3.25 Hz, CH_3). IR (cm^{-1}): $\tilde{\nu}$ = 3058 (s; $\nu(C-H_{arom})$), 2987 (s; $\nu(C-H_{aliph})$), 2957 (s; $\nu(C-H_{aliph})$), 1610 (m), 1505 (m), 1456 (m), 1358 (s; $\nu(SO_2-N)$), 1158 (s; $\nu(SO_2-N)$), 1124 (s; ν(C−F)), 1058 (s), 857 (s). HRMS (ESI): m/z calcd for $C_{13}H_7F_5NO_2S$ + Na + H^+ [M + Na + H^+]: 360.0088. Found: 360.0089. HPLC analysis: retention time = 11.520 min, peak area, 99.7%. Elemental analysis calcd (%) for $C_{13}H_7F_5NO_2S$: C 46.30, H 2.39, N 4.15, S 9.51. Found: C 46.26, H 2.46, N 4.21, S 9.50.

2′,4′-Difluoro-*N*-methyl-2-thiophenesulfonanilide (**12**). Pale yellow solid; yield 64%; mp 80 °C (EtOH). ^{1}H NMR (500 MHz, $CDCl_3$): δ_H 7.62 (dd, J = 5.04 Hz, 1.03 Hz, 1H), 7.45 (dd, J = 3.97 Hz, 1.03 Hz, 1H), 7.28 (td, J = 8.60 Hz, 5.95 Hz, 1H), 7.11 (dd, J = 5.04 Hz, 3.97 Hz, 1H), 6.87 (tdd, J = 8.19 Hz, 2.95 Hz, 1.55 Hz, 1H), 6.81 (ddd, J = 10.43 Hz, 8.60 Hz, 2.95 Hz, 1H), 3.25 ppm (d, J = 0.94 Hz, 3H). ^{13}C NMR (125 MHz, $CDCl_3$): δ_C 162.53 (dd, J = 251.61 Hz, 11.60 Hz, C−F), 159.75 (dd, J = 255.65 Hz, 12.68 Hz, C−F), 138.10 (C_{quat}), 132.86 (CH−S), 132.67, 132.43 (dd, J = 10.13 Hz, 2.68 Hz, $C-H_{arom}$), 127.71, 124.69 (dd, J = 11.73 Hz, 4.14 Hz, C_{quat}), 111.97 (dd, J = 22.30 Hz, 3.69 Hz, $C-H_{arom}$), 105.28 (dd, J = 26.37 Hz, 23.92 Hz, $C-H_{arom}$), 38.43 ppm (d, J = 3.62 Hz, CH_3). IR (cm^{-1}): $\tilde{\nu}$ = 3110 (s; ν(thiophene)), 3088 (s), 3058 (s; $\nu(C-H_{arom})$), 1504 (m), 1349 (s; $\nu(SO_2-N)$), 1176 (s; $\nu(SO_2-N)$), 1153 (s; ν(C−F)), 720 (s; ν(thiophene)), 683 (s). HRMS (ESI): m/z calcd for $C_{11}H_8F_2NO_2S_2$ + Na + H^+ [M + Na + H^+]: 311.9935. Found: 311.9942. HPLC analysis: retention time = 8.888 min, peak area, 99.3%. Elemental analysis calcd (%) for $C_{11}H_8F_2NO_2S_2$: C 45.67, H 3.14, N 4.84, S 22.16. Found: C 45.56, H 2.95, N 4.96, S 22.25.

SHIP2 Activity Measurements. For the activity measurements and other biological assays, sulfonanilides **1**−**12** were dissolved in DMSO and then further diluted into indicated concentrations in assay buffers or media. The capacities of **1**−**12** to inhibit SHIP2 activity and the IC_{50} values of **1**−**12** were measured using the recombinant SHIP2 phosphatase domain and malachite green phosphate assay at the High Throughput Biomedicine Unit (University of Helsinki, Finland). Different concentrations of **1**−**12** were dispensed to 384-well plates after which 100 ng of purified His-tagged recombinant SHIP2 phosphatase domain in reaction buffer (10 mM HEPES, pH 7.25, 6 mM $MgCl_2$, 0.1% CHAPS, 250 mM sucrose and 0.25

https://dx.doi.org/10.1021/acsomega.9b02944
ACS Omega 2020, 5, 1430−1438

mM EDTA) was added, and the plates were incubated for 15 min at room temperature. The reaction was started by adding 7.5 μL of PI(3,4,5)P3 (Echelon Biosciences, Salt Lake City, UT, USA) diluted in the reaction buffer (the final concentration of PI(3,4,5)P3 per well was 100 μM in the total volume of 15 μL), plates were incubated for 20 min at room temperature, and 15 μL of BIOMOL green reagent (Biomol, Plymouth Meeting, PA, USA) was added to wells. After 25 min incubation at room temperature, the absorbance was measured at 620 nm using a Pherastar FS plate reader (BMG Labtech, Offenburg, Germany) (n = 3 for each condition).

Cell Culture. Rat L6 myoblasts (American Type Culture Collection, Manassas, Virginia, USA) and L6 myoblasts stably overexpressing HA-tagged GLUT4 transporter (L6-GLUT4) were grown in high glucose DMEM (Sigma-Aldrich) supplemented with 10% FBS (Sigma-Aldrich, St. Louis, MO, USA), glutamine (Lonza; Walkersville, MD, USA), and penicillin−streptomycin (Sigma-Aldrich) at +37 °C in a humidified 5% CO_2 atmosphere. For differentiation, the FBS concentration in the medium was lowered to 2%.

Cytotoxicity Assay. For cytotoxicity analyses, L6 myoblasts were seeded on 96-well plates, differentiated for 7 days into myotubes, and incubated O/N with 0-300 μM sulfonanilides after which 10 μL of alamarBlue cell viability reagent (ThermoFisher Scientific, Waltham, MA, USA) was added according to the manufacturer instructions. The fluorescence was measured at 544/590 nm ± 20 nm using a Hidex Sense microplate reader (Hidex, Turku, Finland) at 0 and 60 min time points after the addition of the alamarBlue reagent, and the viability of the cells was calculated. The assay was repeated three times (n = 4 for each condition).

Akt Activation Assay. To measure the Akt activation (phosphorylation), L6 myoblasts were differentiated into myotubes for 7 days, serum starved O/N, and treated with 0−50 μM sulfonanilides for 15 min after which 10 nM insulin (Actrapid, Novo Nordisk, Bagsvaerd, Denmark) was added for an additional 15 min. The cells were lysed in NP-40 buffer (1% nonidet P-40, 20 mM Tris−HCl pH 7.4, 150 mM NaCl) supplemented with phosphatase inhibitors (50 mM NaF and 1 mM Na_3VO_4) and protease inhibitor cocktail (cOmpleteProtease Inhibitor Coctail tablets, Roche Diagnostics GmbH, Mannheim, Germany) and then immunoblotted as in Tolvanen et al.[32] Briefly, samples were separated in 8% polyacrylamide gels and transferred onto PVDF membrane (Immobilon-FL PVDF transfer membrane, Merck Millipore Ltd., Tullagreen, Ireland). The membrane was blocked using Odyssey blocking buffer (LI-COR, Lincoln, NE, USA) and incubated with primary antibodies against pAkt (phospho-Akt, Ser473, #9271, Cell Signaling Technology, Danvers, MA, USA), Akt (pan-Akt, #281046, R&D Systems, Minneapolis, MN, USA), and actin (A3853, Sigma-Aldrich) followed by secondary antibodies (IRDye 800CW Donkey anti-Rabbit and IRDye 680RD Donkey anti-Mouse, both from LI-COR, Lincoln, NE, USA). Three individual assays were performed (n = 3 for each condition).

Glucose Uptake Assay. Glucose uptake was measured by a radioactive 2-deoxyglucose assay. L6 myotubes overexpressing GLUT4 glucose transporter were differentiated for 8−9 days. Cells were serum-starved for 20 h supplemented with 50 μM of sulfonanilides **10** or **11**, 50 μM of metformin. Thereafter, cells were stimulated or not with 100 nM insulin for 15 min at 37 °C in DMEM (without D-glucose, L-glutamine, phenol red, and sodium pyruvate) (Gibco/Thermo Fisher Scientific). The cells were exposed to 1 μCi/mL 2-deoxy-D-[1, 2-$^3H(N)$]-glucose (PerkinElmer, Waltham MA, USA) for 5 min at 37 °C. Cells were lysed in 1% Triton X-100 in PBS, and the radioactivity of lysates was measured with a Wallac 1450 Microbeta Trilux liquid scintillator and a luminescense counter (PerkinElmer). Four independent experiments were performed, with 4 technical replicates for each condition.

On-Cell Western for HA-GLUT4. Differentiated L6-GLUT4 myotubes cultured on 96-well plate were treated with sulfonanilides **10** or **11** at 50 μM concentration for 20 h, of which the last 4 h in a serum-free medium. The quiescent cells were stimulated or not with 100 nM insulin for 15 min at 37 °C and fixed with 2% paraformaldehyde on ice for 5 min followed by 20 min at room temperature. The cells were incubated with a primary antibody against HA.11 epitope tag (#901513, BioLegend, San Diego, CA, USA) diluted 1/100 in 50% Odyssey Blocking buffer (LI-COR) in PBS at room temperature for 1 h, followed by incubation with a secondary antibody (IRDye 800CW Donkey anti-Mouse, LI-COR) and the nuclear marker DRAQ-5 (Thermo Fisher Scientific, Rockford, IL, USA) at room temperature for 1 h. The fluorescent signals were detected and quantified with an Odyssey infrared imager (LI-COR). DRAQ-5 was used for normalization. Four independent experiments were performed, resulting in total in 30−34 replicates for each condition.

Statistical Analyses. Data are presented as means ± STD or SEM of three or four independent experiments. Statistical analyses were performed using an unpaired, two-tailed Student's t-test. P-values ≤0.05 were considered statistically significant. IC_{50}-values were calculated using GraphPad Software, Inc., Prism version 6.05 (San Diego, CA, USA) using four-parameter curve-fit.

Molecular Docking of Sulfonanilide 11 onto the Structural Model of SHIP2. The crystal structure of the phosphatase domain of human SHIP2 in complex with a ligand biphenyl 2,3′,4,5′,6-pentakisphosphate was obtained from the Protein Data Bank (PDB ID: 4A9C). The protein structure was cleaned, hydrogens added, and solvent molecules removed using Dassault Systèmes BIOVIA, BIOVIA Discovery Studio, client 2018, San Diego: Dassault Systèmes, 2018, software. Sulfonanilide **11** was prepared using a prepared ligand function. The binding site in SHIP2 was designed as described in Mills et al.[23] Docking of **11** onto the model of SHIP2 was performed using GOLD 5.7.1 with default parameters, and the docking poses were analyzed visually and based on the Goldscore Fitness values.

■ ASSOCIATED CONTENT

Supporting Information

The Supporting Information is available free of charge at https://pubs.acs.org/doi/10.1021/acsomega.9b02944.

All ^{1}H-, ^{13}C-NMR spectra and HPLC chromatograms of the synthesized sulfonanilides **1**−**12** (PDF)

Crystal structure of human SHIP2 in complex with biphenyl 2,3′,4,5′,6-pentakisphosphate (PDB)

■ AUTHOR INFORMATION

Corresponding Author

Kristiina Wähälä − *University of Helsinki, Helsinki, Finland;* orcid.org/0000-0003-4082-8622;

https://dx.doi.org/10.1021/acsomega.9b02944
ACS Omega 2020, 5, 1430−1438

Phone: +358504487502; Email: kristiina.wahala@helsinki.fi

Other Authors

Mika E. A. Berg − *University of Helsinki, Helsinki, Finland;* orcid.org/0000-0002-1095-0179

Jette-Britt Naams − *University of Helsinki, Helsinki, Finland*

Laura C. Hautala − *University of Helsinki, Helsinki, Finland*

Tuomas A. Tolvanen − *University of Helsinki, Helsinki, Finland*

Jari P. Ahonen − *University of Helsinki, Helsinki, Finland*

Sanna Lehtonen − *University of Helsinki, Helsinki, Finland;* orcid.org/0000-0003-4189-2415

Complete contact information is available at: https://pubs.acs.org/10.1021/acsomega.9b02944

Author Contributions

#J.-B.N. and L.C.H. contributed equally. M.E.A.B. and J.P.A. synthesized and analyzed all the sulfonanilide inhibitors. M.E.A.B. carried out the computational studies. J.-B.N., L.C.H., T.A.T., and S.L. carried out the biological testing of the sulfonanilide inhibitors. M.E.A.B., J.-B.N., and K.W. wrote the manuscript, and all co-authors corrected the manuscript.

Notes

The authors declare no competing financial interest.

■ ACKNOWLEDGMENTS

Business Finland (to S.L. and K.W.) and the Jane and Aatos Erkko Foundation (to S.L.) are thanked for financial support. CSC Computer Service Center is acknowledged for providing computer time.

■ REFERENCES

(1) *IDF Diabetes Atlas*; International Diabetes Federation, 8th Ed., 2017, p. 9.

(2) American Diabetes Association. Diagnosis and Classification of Diabetes Mellitus. *Diabetes Care* **2014**, *37*, S81−S90.

(3) Pratley, R. E. The Early Treatment of Type 2 Diabetes. *Am. J. Med.* **2013**, *126*, S2−S9.

(4) Chatterjee, S.; Khunti, K.; Davies, M. J. Type 2 Diabetes. *Lancet* **2017**, *389*, 2239−2251.

(5) Ahlqvist, E.; Storm, P.; Käräjämäki, A.; Martinell, M.; Dorkhan, M.; Carlsson, A.; Vikman, P.; Prasad, R. B.; Aly, D. M.; Almgren, P.; Wessman, Y.; Shaat, N.; Spégel, P.; Mulder, H.; Lindholm, E.; Melander, O.; Hansson, O.; Malmqvist, U.; Lernmark, Å.; Lahti, K.; Forsén, T.; Tuomi, T.; Rosengren, A. H.; Groop, L. Novel Subgroups of Adult-Onset Diabetes and Their Association with Outcomes: A Data-Driven Cluster Analysis of Six Variables. *Lancet Diabetes Endocrinol.* **2018**, *6*, 361−369.

(6) Pessin, J. E.; Saltiel, A. R. Signaling Pathways in Insulin Action: Molecular Targets of Insulin Resistance. *J. Clin. Invest.* **2000**, *106*, 165−169.

(7) Jaldin-Fincati, J. R.; Pavarotti, M.; Frendo-Cumbo, S.; Bilan, P. J.; Klip, A. Update on GLUT4 Vesicle Traffic: A Cornerstone of Insulin Action. *Trends Endocrinol. Metab.* **2017**, *28*, 597−611.

(8) Wasik, A. A.; Lehtonen, S. Glucose Transporters in Diabetic Kidney Disease—Friends or Foes? *Front. Endocrinol.* **2018**, *9*, 155.

(9) Blero, D.; De Smedt, F.; Pesesse, X.; Paternotte, N.; Moreau, C.; Payrastre, B.; Erneux, C. The SH2 Domain Containing Inositol 5-Phosphatase SHIP2 Controls Phosphatidylinositol 3,4,5-Trisphosphate Levels in CHO-IR Cells Stimulated by Insulin. *Biochem. Biophys. Res. Commun.* **2001**, *282*, 839−843.

(10) Wada, T.; Sasaoka, T.; Funaki, M.; Hori, H.; Murakami, S.; Ishiki, M.; Haruta, T.; Asano, T.; Ogawa, W.; Ishihara, H.; Kobayashi, M. Overexpression of SH2-Containing Inositol Phosphatase 2 Results in Negative Regulation of Insulin-Induced Metabolic Actions in 3T3-L1 Adipocytes via Its 5′-Phosphatase Catalytic Activity. *Mol. Cell. Biol.* **2001**, *21*, 1633−1646.

(11) Marion, E.; Kaisaki, P. J.; Pouillon, V.; Gueydan, C.; Levy, J. C.; Bodson, A.; Krzentowski, G.; Daubresse, J.-C.; Mockel, J.; Behrends, J.; Servais, G.; Szpirer, C.; Kruys, V.; Gauguier, D.; Schurmans, S. The Gene INPPL1, Encoding the Lipid Phosphatase SHIP2, Is a Candidate for Type 2 Diabetes in Rat and Man. *Diabetes* **2002**, *51*, 2012−2017.

(12) Kaisaki, P. J.; Delepine, M.; Woon, P. Y.; Sebag-Montefiore, L.; Wilder, S. P.; Menzel, S.; Vionnet, N.; Marion, E.; Riveline, J.-P.; Charpentier, G.; Schurmans, S.; Levy, J. C.; Lathrop, M.; Farrall, M.; Gauguier, D. Polymorphisms in Type II SH2 Domain-Containing Inositol 5-Phosphatase (INPPL1, SHIP2) Are Associated With Physiological Abnormalities of the Metabolic Syndrome. *Diabetes* **2004**, *53*, 1900−1904.

(13) Kagawa, S.; Sasaoka, T.; Yaguchi, S.; Ishihara, H.; Tsuneki, H.; Murakami, S.; Fukui, K.; Wada, T.; Kobayashi, S.; Kimura, I.; Kobayashi, M. Impact of Src Homology 2-Containing Inositol 5′-Phosphatase 2 Gene Polymorphisms Detected in a Japanese Population on Insulin Signaling. *J. Clin. Endocrinol. Metab.* **2005**, *90*, 2911−2919.

(14) Ishida, S.; Funakoshi, A.; Miyasaka, K.; Shimokata, H.; Ando, F.; Takiguchi, S. Association of SH-2 Containing Inositol 5′-Phosphatase 2 Gene Polymorphisms and Hyperglycemia. *Pancreas* **2006**, *33*, 63−67.

(15) Hyvönen, M. E.; Ihalmo, P.; Forsblom, C.; Thorn, L.; Sandholm, N.; Lehtonen, S.; Groop, P.-H. INPPL1 is Associated with the Metabolic Syndrome in Men with Type 1 Diabetes, but Not with Diabetic Nephropathy. *Diabetic Med.* **2012**, *29*, 1589−1595.

(16) Hori, H.; Sasaoka, T.; Ishihara, H.; Wada, T.; Murakami, S.; Ishiki, M.; Kobayashi, M. Association of SH2-Containing Inositol Phosphatase 2 With the Insulin Resistance of Diabetic Db/Db Mice. *Diabetes* **2002**, *51*, 2387−2394.

(17) Hyvönen, M. E.; Saurus, P.; Wasik, A.; Heikkilä, E.; Havana, M.; Trokovic, R.; Saleem, M.; Holthöfer, H.; Lehtonen, S. Lipid Phosphatase SHIP2 Downregulates Insulin Signalling in Podocytes. *Mol. Cell. Endocrinol.* **2010**, *328*, 70−79.

(18) Suwa, A.; Kurama, T.; Yamamoto, T.; Sawada, A.; Shimokawa, T.; Aramori, I. Glucose Metabolism Activation by SHIP2 Inhibitors via Up-Regulation of GLUT1 Gene in L6 Myotubes. *Eur. J. Pharmacol.* **2010**, *642*, 177−182.

(19) Suwa, A.; Yamamoto, T.; Sawada, A.; Minoura, K.; Hosogai, N.; Tahara, A.; Kurama, T.; Shimokawa, T.; Aramori, I. Discovery and Functional Characterization of a Novel Small Molecule Inhibitor of the Intracellular Phosphatase, SHIP2. *Br. J. Pharmacol.* **2009**, *158*, 879−887.

(20) Ichihara, Y.; Fujimura, R.; Tsuneki, H.; Wada, T.; Okamoto, K.; Gouda, H.; Hirono, S.; Sugimoto, K.; Matsuya, Y.; Sasaoka, T.; Toyooka, N. Rational Design and Synthesis of 4-Substituted 2-Pyridin-2-Ylamides with Inhibitory Effects on SH2 Domain-Containing Inositol 5′-Phosphatase 2 (SHIP2). *Eur. J. Med. Chem.* **2013**, *62*, 649−660.

(21) Sasaoka, T.; Tsuneki, H.; Wada, T.; Toyooka, N.; Hirono, S.; Gota, H. (Benzenesulfonylamino) benzamide Derivative, and SHIP2 Inhibitor Containing same as Active Ingredient. International Patent WO 2015/016293 A1, February 5, 2015.

(22) Polianskyte-Prause, Z.; Tolvanen, T. A.; Lindfors, S.; Dumont, V.; Van, M.; Wang, H.; Dash, S. N.; Berg, M.; Naams, J.-B.; Hautala, L. C.; Nisen, H.; Mirtti, T.; Groop, P.-H.; Wähälä, K.; Tienari, J.; Lehtonen, S. Metformin Increases Glucose Uptake and Acts Renoprotectively by Reducing SHIP2 Activity. *FASEB J.* **2018**, *33*, 2858−2869.

(23) Mills, S. J.; Persson, C.; Cozier, G.; Thomas, M. P.; Trésaugues, L.; Erneux, C.; Riley, A. M.; Nordlund, P.; Potter, B. V. L. A Synthetic Polyphosphoinositide Headgroup Surrogate in Complex with SHIP2

Provides a Rationale for Drug Discovery. *ACS Chem. Biol.* **2012**, *7*, 822−828.
(24) Springer, J. E.; Azbill, R. D.; Carlson, S. L. A Rapid and Sensitive Assay for Measuring Mitochondrial Metabolic Activity in Isolated Neural Tissue. *Brain Res. Protoc.* **1998**, *2*, 259−263.
(25) Rampersad, S. N. Multiple Applications of Alamar Blue as an Indicator of Metabolic Function and Cellular Health in Cell Viability Bioassays. *Sensors* **2012**, *12*, 12347−12360.
(26) Hundal, H. S.; Ramlal, T.; Reyes, R.; Leiter, L. A.; Klip, A. Cellular Mechanism of Metformin Action Involves Glucose Transporter Translocation from an Intracellular Pool to the Plasma Membrane in L6 Muscle Cells. *Endocrinology* **1992**, *131*, 1165−1173.
(27) Viollet, B.; Guigas, B.; Garcia, N. S.; Leclerc, J.; Foretz, M.; Andreelli, F. Cellular and Molecular Mechanisms of Metformin: An Overview. *Clin. Sci.* **2012**, *122*, 253−270.
(28) Proks, P.; Reimann, F.; Green, N.; Gribble, F.; Ashcroft, F. Sulfonylurea Stimulation of Insulin Secretion. *Diabetes* **2002**, *51*, S368−S376.
(29) Tsiani, E.; Ramlal, T.; Leiter, L. A.; Klip, A.; Fantus, I. G. Stimulation of Glucose Uptake and Increased Plasma Membrane Content of Glucose Transporters in L6 Skeletal Muscle Cells by the Sulfonylureas Gliclazide and Glyburide. *Endocrinology* **1995**, *136*, 2505−2512.
(30) Lee, K. W.; Ku, Y. H.; Kim, M.; Ahn, B. Y.; Chung, S. S.; Park, K. S. Effects of Sulfonylureas on Peroxisome Proliferator-Activated Receptor γ Activity and on Glucose Uptake by Thiazolidinediones. *Diabetes Metab. J.* **2011**, *35*, 340.
(31) Tontonoz, P.; Spiegelman, B. M. Fat and Beyond: The Diverse Biology of PPARγ. *Annu. Rev. Biochem.* **2008**, *77*, 289−312.
(32) Tolvanen, T. A.; Dash, S. N.; Polianskyte-Prause, Z.; Dumont, V.; Lehtonen, S. Lack of CD2AP Disrupts Glut4 Trafficking and Attenuates Glucose Uptake in Podocytes. *J. Cell Sci.* **2015**, *128*, 4588−4600.

https://dx.doi.org/10.1021/acsomega.9b02944
ACS Omega 2020, 5, 1430−1438